

PCCP

Accepted Manuscript



This is an *Accepted Manuscript*, which has been through the Royal Society of Chemistry peer review process and has been accepted for publication.

Accepted Manuscripts are published online shortly after acceptance, before technical editing, formatting and proof reading. Using this free service, authors can make their results available to the community, in citable form, before we publish the edited article. We will replace this *Accepted Manuscript* with the edited and formatted *Advance Article* as soon as it is available.

You can find more information about *Accepted Manuscripts* in the [Information for Authors](#).

Please note that technical editing may introduce minor changes to the text and/or graphics, which may alter content. The journal's standard [Terms & Conditions](#) and the [Ethical guidelines](#) still apply. In no event shall the Royal Society of Chemistry be held responsible for any errors or omissions in this *Accepted Manuscript* or any consequences arising from the use of any information it contains.

FRET versus PET: ratiometric chemosensors assembled from naphthalimide dyes and crown ethers

Pavel A. Panchenko^{a,b,*}, Yuri V. Fedorov^a, Olga A. Fedorova^{a,b}, Gediminas Jonusauskas^c

^a*A. N. Nesmeyanov Institute of Organoelement Compounds of Russian Academy of Sciences (INEOS RAS), 119991, Vavilova str. 28, Moscow, Russia,
Tel.: +7 499 135 80 98, Fax: +7 499 135 50 85, E-mail: pavel@ineos.ac.ru*

^b*D. Mendeleev University of Chemical Technology of Russia,
125047, Miusskaya sq. 9, Moscow, Russia,*

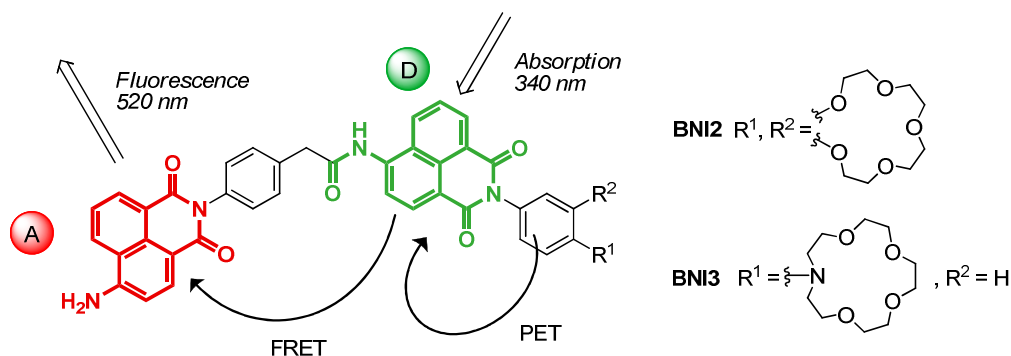
^c*Laboratoire Ondes et Matière d'Aquitaine (LOMA), UMR CNRS 5798,
Bordeaux University, 33405, 351 Cours de la Libération, Talence, France*

Abstract

Novel bi-chromophoric naphthalimide derivatives containing benzo-15-crown-5 and *N*-phenyl-aza-15-crown-5 receptor moieties **BNI2** and **BNI3** were designed and prepared. Significant Förster resonance energy transfer (FRET) from donor (D) amido-naphthalimide to acceptor (A) amino-naphthalimide chromophore as well as photoinduced electron transfer (PET) between the *N*-aryl receptor and amido-naphthalimide fragment were revealed by the steady-state and time resolved UV/Vis absorption and fluorescence spectroscopy. Upon the addition of alkaline-earth metal perchlorates to an acetonitrile solution of ligands, FRET mediated fluorescence enhancement was observed, which was a result of inhibition of PET competitive deactivation pathway. The studied compounds provide an opportunity to register two-channel fluorescence response using selective excitation of either of the photoactive units and, thus might be of interest as ratiometric probes.

Keywords: 1,8-naphthalimide, crown compounds, sensors, photoinduced electron transfer (PET), Förster resonance energy transfer (FRET).

Graphical Abstract



Textual abstract for the table of contents entry

Crown-containing naphthalimide dyads exhibited ratiometric fluorescence response to the presence of metal cations and protons resulting from the competition between PET and FRET processes.

1. Introduction

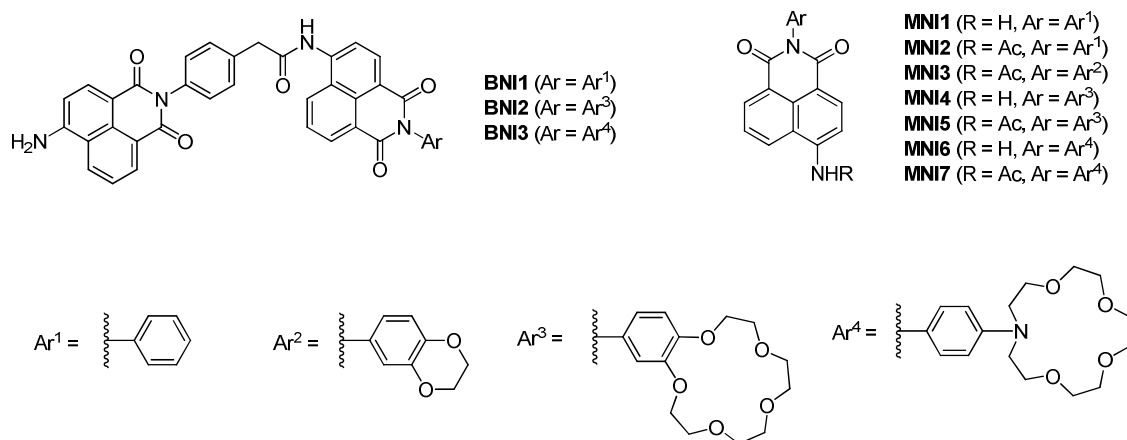
Förster resonance energy transfer is a unique process making possible to generate fluorescence signals sensitive to molecular conformation, association and separation in the 1–10 nm range.^{1,2} This mechanism has been widely used in medicinal diagnostics, optical imaging and molecular biology as a spectroscopic ruler to study structure of proteins and nucleic acids. In recent years, significant emphasis has been placed on the development of highly selective fluorescent FRET based chemosensors for metal cations because of their potential applications in biochemistry and environmental research. Among various photoinduced processes that are commonly involved in the signaling or response phenomena, the resonance energy transfer seems to be an optimal strategy for designing ratiometric probes.^{3,4}

According to ratiometric method, analyte concentration can be quantified by using the ratio of intensities of the well resolved fluorescence peaks with reasonable intensities at two different wavelengths for analyte free and analyte bound probe.⁵ Such self-calibration using two emission bands can eliminate the influence of indicator dye concentration, environmental conditions and instrumental efficiency. Furthermore, the pseudo-Stokes shifts of FRET based probes are larger than the Stokes shifts of either the donor or acceptor dyes; thus, the possible self-quenching as well as fluorescence detection errors due to back scattering effects from the excitation source will be efficiently avoided.⁶

Naphthalimide derivatives are a special class of environmentally sensitive fluorophores. The fluorescence of 1,8-naphthalimides with electron donating groups at C-4 position of naphthalene ring has been of great interest for several decades in connection with an array of technical, medical and electronic use. Because of its intense fluorescence and good photostability, this type of compounds has found application in a number of areas including coloration of polymers,^{7,8} laser active media,^{9,10} fluorescent markers in biology,^{11–13} anticancer agents and analgesics in medicine,¹⁴ electroluminescent materials,^{15–17} fluorescence switchers,^{18–20} liquid crystal displays^{21,22} and ion probes.^{23,24}

To date some examples of naphthalimide based FRET probes have been reported in literature. Georgiev et al. described synthesis and pH-sensitive fluorescence of PAMAM dendrons core and peripherally functionalized with amino- and alkoxy-naphthalimides as donor and acceptor fluorophores.^{25–27} A FRET-based ratiometric chemosensor for in vitro cellular fluorescence analyses of pH based on naphthalimide–coumarin system was reported by Zhou et al.²⁸ Selective ratiometric chemosensors for Cu²⁺ and Zn²⁺ were obtained using dansylamide–naphthalimide conjugates with variable polymethylene linker length between the chromophores.^{29,30} A few chemosensors for metal cations and protons containing amino-naphthalimide and rhodamine units in which spirolactam to ring-open amide equilibrium of

rhodamine dyes is used to switch FRET from the amino-naphthalimide fragment were studied.³¹⁻⁴⁰



Scheme 1. Structure of compounds **MNI1–7** and **BNI1–3**

We recently developed monochromophoric amino- and amido-naphthalimide derivatives **MNI4–6** (Scheme 1) bearing crown ether groups as fluorescent sensors exploiting process of photoinduced electron transfer.^{41–43} These compounds displayed pronounced enhancement of emission intensity by coordination with metal cations, which was a result of inhibition of PET between crown ether receptor conjugated with *N*-phenyl ring and fluorophore. Herein, we report the design, synthesis and investigation of cation-dependent behavior of FRET-based ratiometric sensors **BNI2–3** by integrating amido-naphthalimide probes **MNI5** and **MNI7** as FRET donors and amino-naphthalimide **MNI1** as an FRET acceptor. In this case, the strategy for detection of metal ions is based on modulating of FRET process, and thus emission intensity of acceptor amino-naphthalimide fragment, by means of incorporation of competitive PET deactivation pathway. In order to receive more complete comparative picture for the influence of crown ether groups on the efficiency of FRET interaction in a bi-chromophoric system we prepared non-ionophoric dyad compound **BNI1**. Naphthalimides **MNI1**,⁴⁴ **MNI2**,⁴⁴ **MNI3**,⁴⁴ **MNI5**⁴⁴ and **MNI7**⁴³ have been synthesized earlier and were also included in photophysical studies as reference compounds.

2. Experimental Section

Steady-state optical measurements. The absorption spectra were taken on a Varian-Cary 5G spectrophotometer. The fluorescence quantum yield measurements were performed using a Varian-Cary 5G spectrophotometer and a FluoroMax-3 spectrofluorimeter. Spectral measurements were carried out in air-saturated acetonitrile solutions (acetonitrile of spectrophotometric grade, water content <0.005%, Aldrich) at 20 ± 1 °C; the concentrations of studied compounds were of about $0.5\text{--}2.0 \cdot 10^{-5}$ M. All measured fluorescence spectra were

corrected for the nonuniformity of detector spectral sensitivity. Coumarin 481 in acetonitrile ($\phi^{\text{fl}} = 0.08$)⁴⁵ was used as reference for the fluorescence quantum yield measurements. The fluorescence quantum yields were calculated by the Eq. (1),⁴⁶

$$\phi_i^{\text{fl}} = \phi_0^{\text{fl}} \frac{S_i(1 - 10^{-A_0})n_1^2}{S_0(1 - 10^{-A_i})n_0^2} \quad (1)$$

wherein ϕ_i^{fl} and ϕ_0^{fl} are the fluorescence quantum yields of the studied solution and the standard compound, respectively; A_i and A_0 are the absorptions of the studied solution and the standard, respectively; S_i and S_0 are the areas underneath the curves of the fluorescence spectra of the studied solution and the standard, respectively; and n_i and n_0 are the refraction indices of the solvents for the substance under study and the standard compound ($n_i = n_0 = 1.342$, acetonitrile).

Time-Resolved Fluorescence Setup. A Ti:sapphire laser system emitting pulses of 0.6 mJ and 30 fs at 800 nm and 1 kHz pulse repetition rate (Femtopower Compact Pro) with home-built optical parametric generator and frequency mixers was used to excite the samples at the maximum of the steady-state absorption band. All excited-state lifetimes were obtained by using depolarized excitation light. The highest pulse energies used to excite fluorescence did not exceed 100 nJ and the average power of excitation beam was 0.1 mW at a pulse repetition rate of 1 kHz focused into a spot with a diameter of 0.1 mm in the 10 mm-long fused-silica cell. The fluorescence emitted in the forward direction was collected by reflective optics and focused with a spherical mirror onto the input slit of a spectrograph (Chromex 250) coupled to a streak camera (Hamamatsu 5680 equipped with a fast single sweep unit M5676, temporal resolution 2 ps). Convolution of a rectangular streak camera slit in the sweep range of 250 ps with electronic jitter of the streak camera trigger pulse provided a Gaussian (over four decades) temporal apparatus function with a full width at half-maximum of 20 ps. The fluorescence kinetics were later fitted by means of the Levenberg–Marquardt least-squares curve-fitting method using a solution of the differential equation describing the evolution in time of a single excited state and neglecting depopulation of the ground state according to Eq. (2),

$$\frac{dI}{dt} = \text{Gauss}(t_0, \Delta t, A) - \frac{I(t)}{\tau} \quad (2)$$

where $I(t)$ is the fluorescence intensity, *Gauss* is the Gaussian profile of the excitation pulse, in which t_0 is the excitation pulse arrival delay, Δt – the excitation pulse width, and A – the amplitude. The parameter τ is the lifetime of the excited state. The initial condition for the equation is $I(-\infty) = 0$. Typically, the fit shows a χ^2 value (Pirson's criteria) better than 10^{-4} and a correlation coefficient $R > 0.999$. The uncertainty of the lifetime was better than 1%. Routinely, the fluorescence accumulation time in our measurements did not exceed 90 s.

Transient Absorption Setup. The laser system and frequency-conversion apparatus employed to excite samples were the same as for time-resolved fluorescence measurements. White light continuum (360–1000 nm) pulses generated in a 5 mm methanol cell were used as a probe. The variable delay time between excitation and probe pulses was obtained by using a delay line with 0.1 mm resolution. The solutions were placed in a 1 mm circulating cell. Whitelight signal and reference spectra were recorded with a two-channel fiber spectrometer (Avantes Avaspec-2048-2). A home-written acquisition and experiment-control program in LabView made it possible to record transient spectra with an average error of less than 10^{-4} times the optical density for all wavelengths. The temporal resolution of our setup was better than 60 fs. Temporal chirp of the probe pulse was corrected by a computer program with respect to a Lorentzian fit of a Kerr signal generated in a 0.2 mm glass plate used in a place of the sample.

Equilibrium constant determination. Complex formation of compounds **BNI2** and **BNI3** with Mg^{2+} and Ca^{2+} in acetonitrile at 20 ± 1 °C was studied by spectrofluorometric titration.^{47,48} The ratio of dye to M^{2+} was varied by adding aliquots of a solution of metal perchlorate* of known concentration to a solution of ligand **BNI2** or **BNI3** of known concentration. The fluorescence spectrum of each solution was recorded, and the stability constants of the complexes were determined using the SPECFIT/32 program (Spectrum Software Associates, West Marlborough, MA). The following equilibria were considered in the fitting (Eq. (3) and Eq. (4), $\text{L} = \text{BNI2}$ or **BNI3**; $\text{M}^{2+} = \text{Mg}^{2+}$ or Ca^{2+}):



In doing so, it was found that the experimental data corresponded to the theoretical ones if only the Eq. (3) was taken into account and the formation of the complexes with composition of 2 : 1 was not observed.

The equilibrium constants for protonation of ligand **BNI3** was not determined by this method because of high stability ($K > 10^7 \text{ M}^{-1}$) of protonated form $(\text{BNI3}) \cdot \text{H}^+$.

Determination of fluorescence quantum yields of complexes. The fluorescence quantum yields of complexes $(\text{BNI2}) \cdot \text{Mg}^{2+}$ and $(\text{BNI3}) \cdot \text{Ca}^{2+}$ were determined using solutions of ligands **BNI2–3** in CH_3CN containing an excess of the corresponding metal perchlorate in order to obtain 90-95% of ligand bound with the cation. The required $\text{M}(\text{ClO}_4)_2$ excess was calculated from the known stability constants using the SPECFIT/32 program. The measurement of ϕ^{fl} for

* Calcium perchlorate for complexation studies was dried in vacuum (7–8 mm Hg) at 240 °C and kept anhydrous over P_2O_5 in desiccator (Caution! Calcium perchlorate may explode when heating. It decomposes at 270 °C⁴⁹). Anhydrous magnesium perchlorate was used as received.

(**BNI3**)·H⁺ was done in the presence of 2 eq. HClO₄ in ligand solutions, which can be understood from the fact that the further addition of HClO₄ did not result in the fluorescence enhancement and complex formation had already been finished.

3. Results and discussion

3.1. Design and synthesis of the compounds

Following the classical description of FRET model, a requirement for efficient energy transfer is that there should be a spectral overlap between the emission of the donor and absorbance of the acceptor dyes. It is well known that absorption and fluorescence characteristics of the 1,8-naphthalimides depend on the nature of the substituent at C-4 position of the 1,8-naphthalimide ring involved in the charge transfer interaction with dicarboximide moiety. In the construction of dyad probes **BNI2–3**, amido-naphthalimide was chosen as an energy donor, because it has strong emission in the visible range centered at 440–460 nm, which covers a part of amino-naphthalimide's absorption ($\lambda_{\max} = 410\text{--}430\text{ nm}$).⁴⁴ Fig. 1 shows the overlap between the absorption and fluorescence spectra of reference compounds **MNI1** and **MNI2** in acetonitrile, fulfilling a favorable condition for FRET.

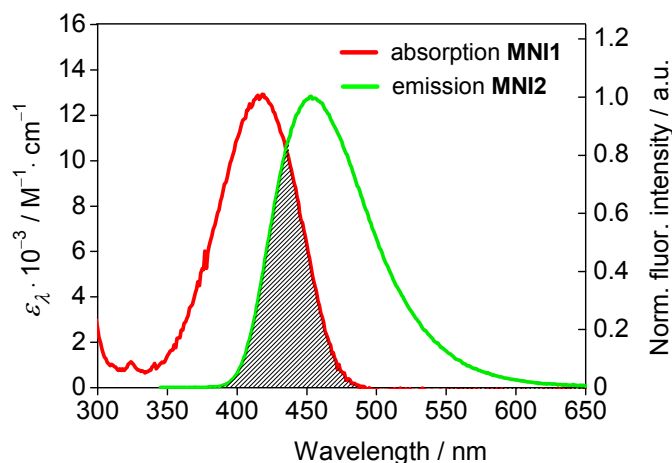
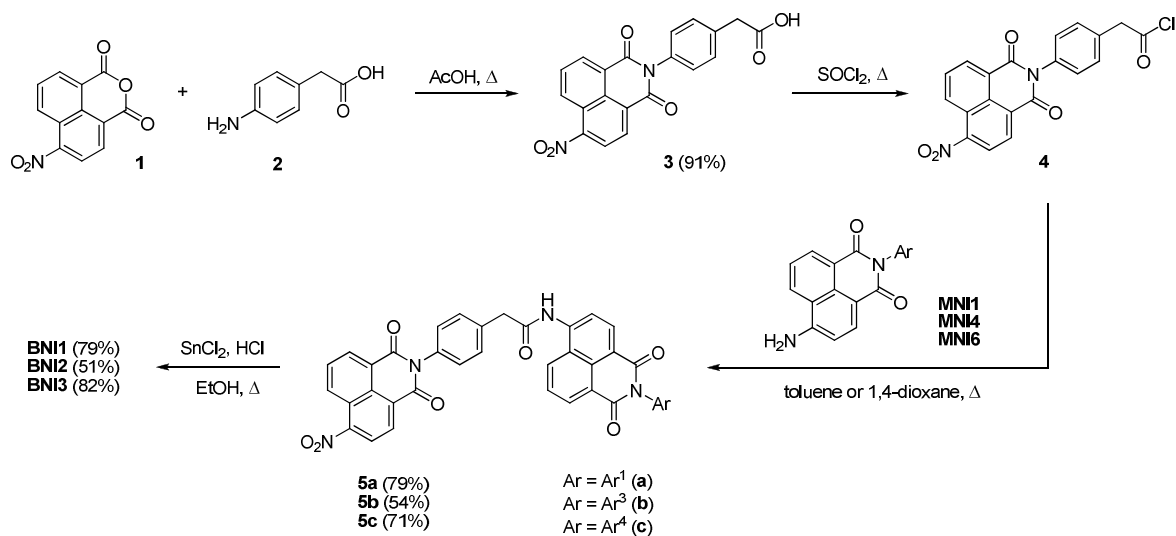


Fig. 1. Overlap between the **MNI1** absorption and **MNI2** emission spectrum in acetonitrile. Concentrations of compounds are both $5.0 \cdot 10^{-6}$ M. Excitation wavelength $\lambda_{\text{ex}} = 340\text{ nm}$.

Another factor, which influences the FRET efficiency is the space separation of donor (D) and acceptor (A) units. Since the transfer rate drops rapidly with the increase of D–A distance, we used rather short and rigid phenyl spacer in **BNI2–3**. Furthermore, low conformational flexibility of phenyl group would also hinder a dyad molecule from adopting a conformation where both naphthalimide moieties are arranged as an internal aggregate stabilized by π -stacking interaction, in which the formation of non-emissive states could be suggested. Crown ether groups were incorporated in the *N*-aryl fragment of more electron deficient amido-

naphthalimide chromophore (in comparison with amino-naphthalimide), because in this case strong PET interaction is expected for both benzo-15-crown-5 and *N*-phenylaza-15-crown-5 ether receptors.^{41,43}



Scheme 2. Synthetic route to compounds BNI1–3

The synthesis of bi-chromophoric naphthalimide derivatives BNI1–3 was carried out using the convergent scheme. Starting from 4-nitronaphthalic anhydride 1, the intermediate 4-nitro-1,8-naphthalimide 3 was afforded by the reaction with (4-aminophenyl)acetic acid in AcOH media (Scheme 2). Compound 3 was refluxed with thionyl chloride to produce chloroanhydride 4, which further was stirred together with preliminary synthetised aminonaphthalimides MNI1, MNI4 and MNI6 in anhydrous toluene or 1,4-dioxane. At the final step, acylation products 5a–c were subjected to reduction using tin (II) chloride in the presence of hydrochloric acid. The experimental details concerning the synthesis of target compounds can be found in Supplementary Information.

3.2. Photophysical properties of the compounds

Photophysical characteristics of BNI1–3 were measured in acetonitrile solution and the data are presented in Table 1. First of all, we studied the resonance energy transfer characteristics of non-crowned derivative BNI1. Absorption spectrum of BNI1 (Fig. 2a), as expected, showed the presence of two long wavelength bands corresponding to the absorption location of amino-naphthalimide donor (reference compound MNI2) and amino-naphthalimide acceptor (reference compound MNI1). Given a high level of additivity of BNI1 spectrum, there could be supposed a lack of any overlap of molecular orbitals between the individual fluorophores in the BNI1 ground state.

Selective excitation of **BNI1** using 340 nm light produced single band emission at 520 nm (Fig. 2b), which is characteristic of amino-naphthalimide fragment.[†] In contrast, under the same conditions, the equimolar mixture of fluorophores **MNI1** and **MNI2** demonstrated the emission at around 450 nm originating from the amido-naphthalimide **MNI2**. This result indicates that in bi-chromophoric system the excitation energy transfers effectively from donor to acceptor unit, whereas in the case of dilute solution of equimolar mixture FRET interaction is not observed.

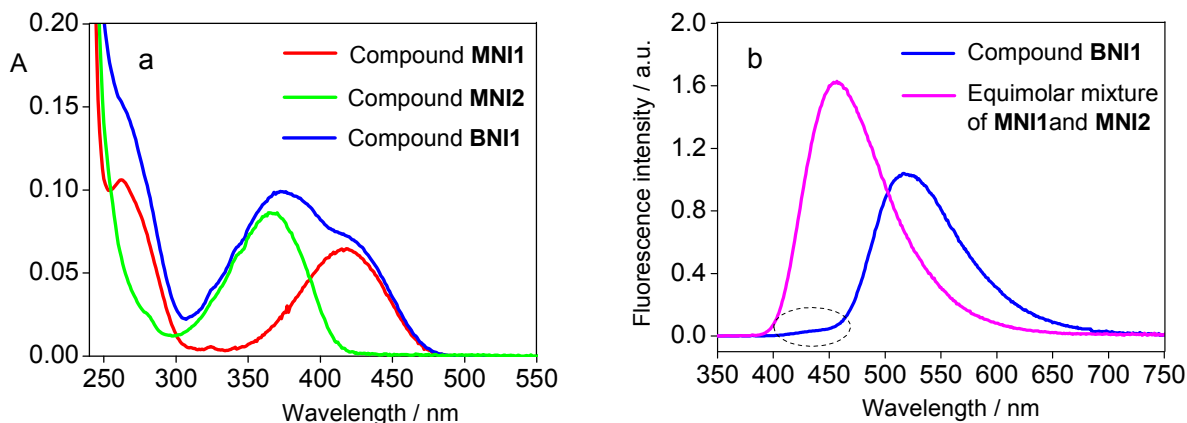


Fig. 2. Absorption spectra of **MNI1**, **MNI2** and **BNI1** (a) and fluorescence spectra of **BNI1** and equimolar mixture of fluorophores **MNI1** and **MNI2** (b) in acetonitrile. Concentration of all compounds is $5.0 \cdot 10^{-6}$ M. Excitation wavelength $\lambda_{\text{ex}} = 340$ nm.

Table 1. Photophysical properties and stability constants of mono- and bi-chromophoric naphthalimides and their complexes in acetonitrile at 20 °C.

Compound	$\lambda_{\text{max}}^{\text{abs}} / \text{nm}$	$\varepsilon_{\lambda} \cdot 10^{-3} / \text{M}^{-1} \cdot \text{cm}^{-1}$	$\lambda_{\text{max}}^{\text{fl}} (\lambda_{\text{ex}}) / \text{nm}$	ϕ^{fl}	$\Phi_{\text{FRET}} / \%$	$\lg K^{\text{a}}$
MNI1	417	12.9	518 (420)	0.55	–	–
MNI2	367	17.3	454 (365)	0.90	–	–
MNI3	366	17.0	454 (365)	0.0048	–	–
MNI5	366	17.4	454 (365)	0.0030	–	–
MNI7	366	15.9	456 (365)	0.0017	–	–
BNI1	371	20.2	520 (340)	0.47	99.997	–
BNI2	368	16.2	520 (340)	0.28	64	–
(BNI2)·Mg²⁺	370	16.9	520 (340)	0.50	–	5.69 ± 0.03
BNI3	368	16.3	519 (340)	0.059	34	–
(BNI3)·Ca²⁺	372	16.6	520 (340)	0.36	–	5.04 ± 0.01
(BNI3)·H⁺	372	15.1	520 (340)	0.45	–	not determined

^aThe dimension of K is M^{-1}

To get deeper insight into the nature of excited state deactivation pathways we measured the excited state lifetime of donor chromophore in the compound **BNI1**. In comparison with the

[†] A weak shoulder at 450 nm in the fluorescence spectrum of **BNI1** results from residual fluorescence of donor chromophore. The appearance of this shoulder can be explained by the relatively high fluorescence quantum yield of **MNI2** (Table 1).

single amidonaphthalimide **MNI2** ($\tau = 10$ ns), it was shorter by more than four orders of magnitude ($\tau_D = 0.31$ ps),[‡] implying the existence of a fast non-radiative process more likely to be the resonance energy transfer. The efficiency of the energy transfer (Φ_{FRET}) in dyad compound **BNI1** was calculated equal to 0.99997 (99.997 %) according to Eq. (5).²

$$EET = 1 - \frac{\tau_D}{\tau} \quad (5)$$

The pretty close value of Φ_{FRET} (99.95%) was obtained from calculations using Förster theory (for details see Supplementary Information). Such high value of Φ_{FRET} could be a result of a rather short distance between donor and acceptor chromophores ($r = 12.0$ Å as obtained from the optimized geometry of **BNI1** (Fig. S1)), which is about 3.5 times shorter compared to critical Förster radius ($R_0 = 41.8$ Å) for this system.

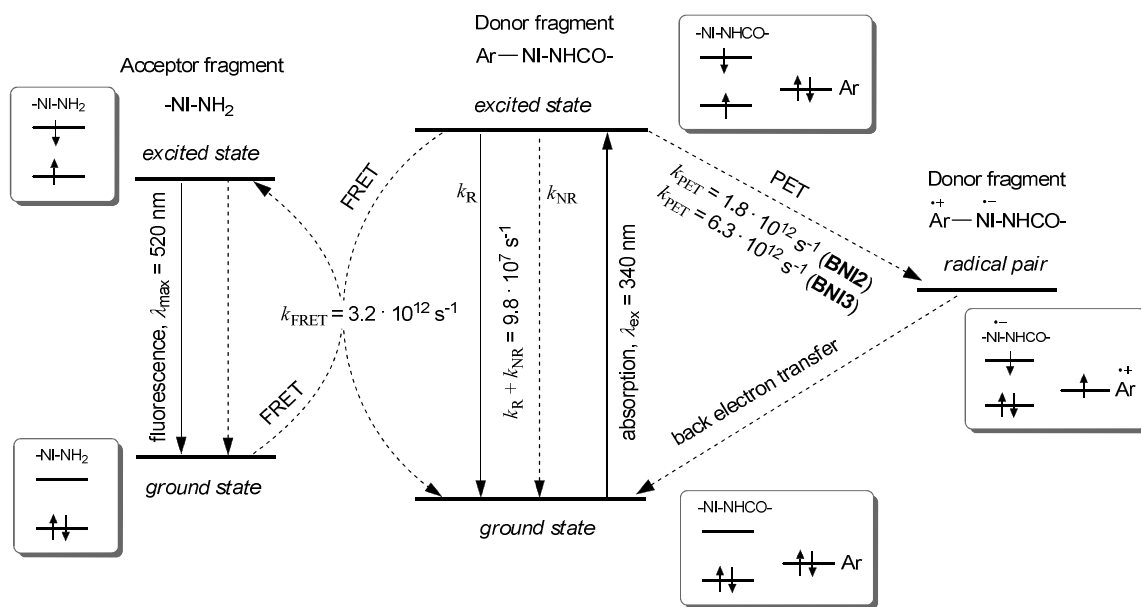


Fig. 3. Excited state relaxation pathways of donor and acceptor chromophores in crown-containing dyads **BNI2** and **BNI3**. Plain and dashed arrows denote radiative and non-radiative processes respectively. Sign «NI» denotes naphthalimide moiety.

The introduction of crown ether substituents in the naphthalimide dyad molecule **BNI1** results in the reduction of the energy transfer efficiency. As it was shown in our previous publications, the presence of electron releasing benzo-15-crown-5-, benzo-1,4-dioxane or *N*-phenyl-aza-15-crown-5 ether groups in the *N*-aryl fragment of amido-naphthalimides **MNI3**, **MNI5** and **MNI7** leads to dramatic decrease of emission intensity with respect to highly emissive non-crowned derivative **MNI2** due to efficient photoinduced electron transfer between the naphthalimide chromophore and receptor moieties.^{41,43,44} Keeping this in mind, one could

[‡] The data for **MNI2** are obtained from the analysis of fluorescence kinetics, for compound **BNI1** – from the analysis of transient absorption spectra (see Experimental Section).

conclude that in the case of crown-containing dyad compounds **BNI2** and **BNI3**, the deactivation of the donor chromophore excited state would proceed via both electron and energy transfer. Additionally, radiative decay (fluorescence) and other possible non-radiative ways of relaxation (except PET and FRET) should be taken into consideration. The representative scheme showing all these energy degradation channels in dyads **BNI2** and **BNI3** is depicted in Fig. 3. Provided each photophysical process in Fig. 3 is characterized by the first order rate constant, the Φ_{FRET} value can be expressed as the ratio of FRET rate constant (k_{FRET}) to the sum of rate constants of all other processes mentioned above (Eq. (6)).

$$\Phi_{\text{FRET}} = \frac{k_{\text{FRET}}}{k_{\text{FRET}} + k_{\text{PET}} + k_{\text{R}} + k_{\text{NR}}} \quad (6)$$

In the Eq. (6), k_{R} stands for the radiative rate constant of amido-naphthalimide chromophore, and k_{NR} describes its non-radiative relaxation which is not related to energy or electron transfer. To estimate the sum ($k_{\text{R}} + k_{\text{NR}}$) we used the value inversely proportional to the fluorescence lifetime of compound **MNI2**, where FRET and PET channels are not realized (Eq. (7)). k_{FRET} was calculated as difference of deactivation rate constants for compounds **BNI1** and **MNI2**, supposing that the decrease of excited state lifetime on going from **MNI2** to **BNI1** is only a result of FRET interaction (Eq. (8)).

$$k_{\text{R}} + k_{\text{NR}} = \frac{1}{\tau} = \frac{1}{10.2 \cdot 10^{-9}} = 9.8 \cdot 10^7 \text{ s}^{-1} \quad (7)$$

$$k_{\text{FRET}} = \frac{1}{\tau_{\text{D}}} - \frac{1}{\tau} = \frac{1}{0.31 \cdot 10^{-12}} - \frac{1}{10.2 \cdot 10^{-9}} = 3.2 \cdot 10^{12} \text{ s}^{-1} \quad (8)$$

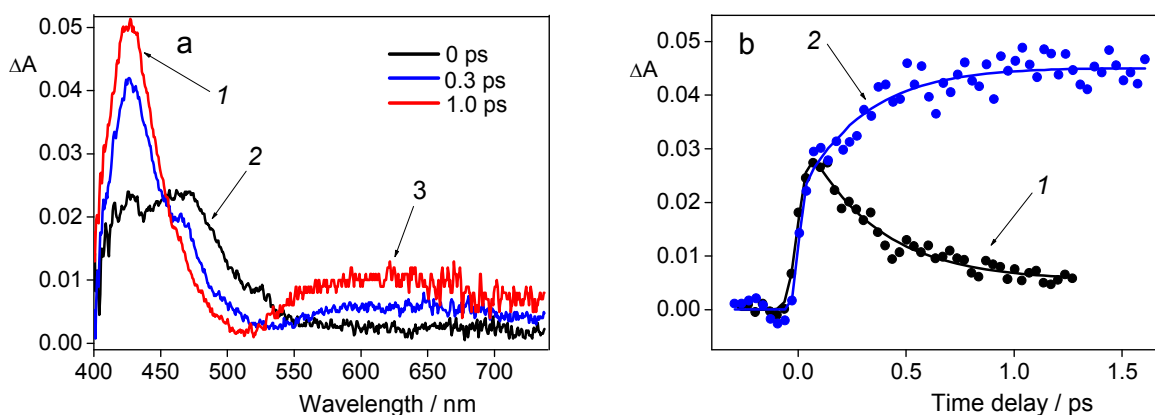


Fig. 4. Transient absorption spectra of **MNI3** at different time delay between pump and probe pulses (a) and transient absorption time profile of **MNI3** (b) in acetonitrile. a) 1 – Absorption band corresponding to cation-radical of benzodioxane fragment; 2 – absorption of singlet S_1 state of amido-naphthalimide chromophore; 3 – possible position of absorption signal of amido-naphthalimide anion-radical. b) 1 – Time profile at absorption maximum of amido-naphthalimide excited S_1 state (480 nm); 2 – Time profile at absorption maximum of benzodioxane cation-radical (420 nm).

Simple analysis of Eq. (6) clearly shows that the FRET efficiency in a bi-chromophoric system can be modulated by changing the rate of photoinduced electron transfer. Thus, the increase of PET donor ability would reduce the amount of energy transferred to amino-naphthalimide acceptor and thereby quench fluorescent output signal. For the evaluation of k_{PET} in dyads **BNI2** and **BNI3**, we used relaxation kinetics data of amido-naphthalimides **MNI3** and **MNI7** in which PET is the main deactivation pathway. As an example, Fig. 4a shows transient absorption spectra of **MNI3** at different time delay between pump and probe pulses. It can be seen that the relaxation of singlet excited state (S_1) proceeds with a concomitant growth of two novel bands probably corresponding to ion-radical intermediates. An intense signal with maximum at 426 nm was assigned by us to benzodioxane cation-radical absorption as it drops into wavelength interval 400 – 480 nm where the characteristic bands of either isomeric dimethoxybenzenes⁵⁰ or *N,N*-dimethylaniline cation-radicals⁵¹ are located. From the analysis of kinetic data (Fig. 4b), PET rate constant (k_{PET}) for the compound **MNI3** was found to be as high as $1.8 \cdot 10^{12} \text{ s}^{-1}$. The similar changes were observed in the transient absorption spectrum of **MNI7** resulting in a k_{PET} value equal to $6.3 \cdot 10^{12} \text{ s}^{-1}$.

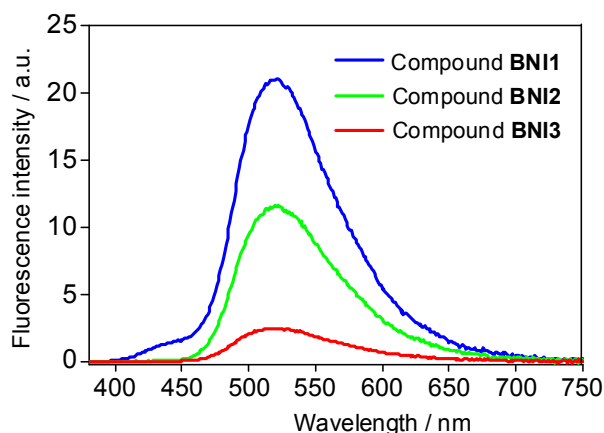


Fig. 5. Fluorescence spectra of compounds **BNI1–3** in acetonitrile. Concentration of all compounds is $6.5 \cdot 10^{-6} \text{ M}$. Excitation wavelength $\lambda_{\text{ex}} = 340 \text{ nm}$.

As the comparison of k_{PET} and k_{FRET} shows, PET and FRET are comparably competing processes. Using the data of time-resolved experiments and Eq. (6), we found that introduction of benzo-15-crown-5 ether receptor into the *N*-phenyl ring of **BNI1** decreases energy transfer efficiency from 99.997% to 64%, whereas the presence of aza-15-crown-5 ether group possessing more strong PET donor ability in the compound **BNI3** results in only 34% of excitation energy involved in FRET. The changes of Φ_{FRET} value in the range of naphthalimide dyads **BNI1–BNI2–BNI3** was found to be in full agreement with the steady-state optical data showing the reduction of the fluorescence intensity and fluorescence quantum yield for the crown-containing compounds (Fig. 5, Table 1).

3.3. Complex formation of naphthalimide dyads

We further examined the ability of crown-containing dyads **BNI2** and **BNI3** to switch their photophysical characteristics as a result of metal ion binding. For the complexation experiments we chose Mg^{2+} and Ca^{2+} , because these cations are known to form stable complexes with benzo-15-crown-5 and aza-15-crown-5 ethers in an acetonitrile solution,^{41,43} which is very convenient when studying cation-induced optical effects.

The addition of magnesium and calcium perchlorates to the solution of ligands **BNI2** and **BNI3** in MeCN doesn't virtually change the position and intensity of the long wavelength absorption bands (compare $\lambda_{\text{max}}^{\text{abs}}$ and ϵ_{λ} values for the free ligands and corresponding complexes in Table 1). This observation indicates that charge transfer transitions in both naphthalimide units in molecules **BNI2** and **BNI3** are not affected by the coordination of metal ions with the crown ether receptors. The similar results were obtained for the monochromophoric naphthalimides **MNI4–7** in our previous publications,^{41,43} where the negligible changes in the absorption spectra were attributed to the lack of conjugation between the *N*-aryl group and naphthalimide chromophore resulted from the nearly orthogonal disposition of these fragments in space. Apparently, the same structural feature persists in dyads **BNI2** and **BNI3** explaining the similarity in spectral behavior.

In contrast to the absorption spectra, the addition of Mg^{2+} and Ca^{2+} led to the pronounced changes in the emission intensity. Considering the ability of PET process to be fully or partially blocked upon the complex formation, one should expect that the binding of metal cations by the **BNI2** and **BNI3** molecules would cause an increase in energy transfer efficiency giving rise to fluorescence enhancement of the acceptor amino-naphthalimide chromophore. As depicted in Fig. 6, the described situation was observed in the experiment. The fluorescence emission spectra of compounds **BNI2** and **BNI3** were recorded in the presence of graduated amounts of corresponding metal perchlorates and the titration data were applied for the calculation of stability constants (Table 1).

From the analysis of cation-induced changes in the emission spectra, it can be seen that optical responses for the compounds **BNI3** and **BNI2** are different and indeed, **BNI3** demonstrates higher extent of fluorescence enhancement. The reason for the observed difference might be explained by the more efficient PET in the free ligand **BNI3**, which intensifies FRET switching contrast. It should, however, be said that the binding of Ca^{2+} by **BNI3** doesn't seem to quench PET interaction completely, because the fluorescence quantum yield of complex (**BNI3**)· Ca^{2+} ($\phi^{\text{fl}} = 0.36$) is somewhat lower as compared to the one of dyad **BNI1** ($\phi^{\text{fl}} = 0.47$) not containing crown ether moiety. Similar results were obtained for complex (**MNI7**)· Ca^{2+} , where sensor properties of monochromophoric naphthalimides **MNI6** and **MNI7** were studied.⁴³

Another factor approving the residual PET in $(\mathbf{BNI3})\cdot\text{Ca}^{2+}$ is that the emission spectrum of the Ca^{2+} -saturated solution of **BNI3** doesn't contain the short wavelength shoulder arose from the fluorescence of donor chromophore which, in contrast, emerges in the case of **BNI1** (Fig. 2b) and $(\mathbf{BNI2})\cdot\text{Mg}^{2+}$ (Fig. 6a).

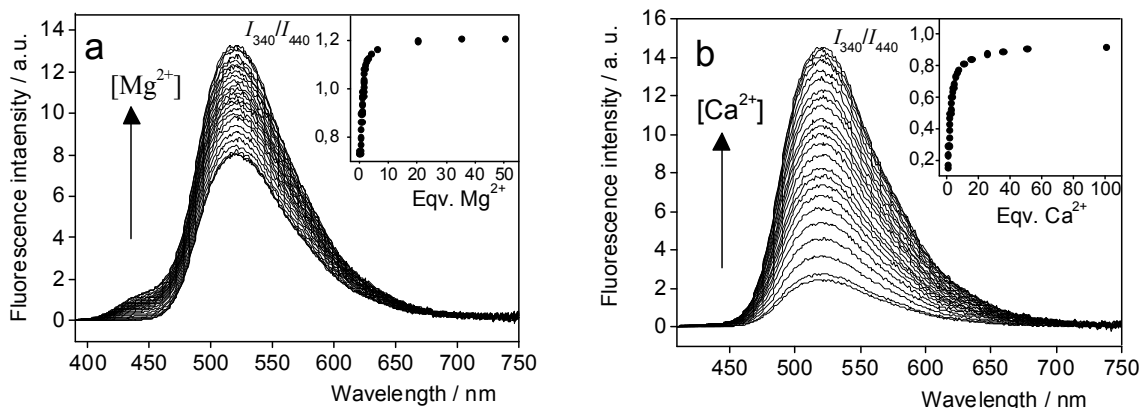


Fig. 6. The changes in the fluorescence spectrum of compound **BNI2** (a) and **BNI3** (b) in acetonitrile solution. Excitation wavelength $\lambda_{\text{ex}} = 340$ nm. The inserts show the ratio of the fluorescence intensity at 520 nm measured using excitation light $\lambda_{\text{ex}} = 340$ nm (I_{340}) to the fluorescence intensity at 520 nm measured using excitation light $\lambda_{\text{ex}} = 440$ nm (I_{440}). a) Concentration of ligand **BNI2** $C_L = 4.5 \cdot 10^{-6}$ M; b) concentration of ligand **BNI3** $C_L = 6.5 \cdot 10^{-6}$ M.

In order to confirm our assumption concerning partial inhibition of PET in the $(\mathbf{BNI3})\cdot\text{Ca}^{2+}$, we measured spectral characteristics of protonated form of ligand **BNI3** (Table 1). The addition of HClO_4 in acetonitrile solutions of **BNI3** resulted in formation of highly fluorescent complexes $(\mathbf{BNI3})\cdot\text{H}^+$ similar in ϕ^{fl} value to **BNI1**. In this complex the lone electron pair of receptor's anilino nitrogen is fully engaged in coordination with the cation due to formation of N–H σ -bond, which breaks the conjugation, significantly lowers the potential energy of *N*-aryl group and thus completely quenches PET process.

Finally, we would like to clear how the studied bi-chromophoric compounds can be applied for the ratiometric detection of ions. The main idea of ratiometric measurements is based on self-calibration of a sensor system. This means that probe's response should contain not only the signal reporting on the analyte binding. There must be a different signal (or signals) that could allow to account or compensate all the effects that influence the fluorescence parameter(s) besides the analyte–probe interaction. In the case of crown-containing dyads **BNI2** and **BNI3**, the excitation of aminonaphthalimide chromophore using the visible light ($\lambda_{\text{ex}} = 440$ nm) leads to emission at 520 nm. Noteworthy, this signal does not depend on whether a cation is present in the crown ether moiety or not and hence, can be used for self-calibration. In contrast, the fluorescence output obtained as a result of donor chromophore excitation with the UV light ($\lambda_{\text{ex}} = 340$ nm) is strongly cation-dependent. Thus, the ratio of the yellow-green emission intensities at 520 nm obtained at $\lambda_{\text{ex}} = 340$ nm and $\lambda_{\text{ex}} = 440$ nm (I_{340}/I_{440}) was found to increase with the

amount of Mg^{2+} or Ca^{2+} added in the solution for both compounds **BNI2** and **BNI3** (Fig. 6, the inserts). This provides an opportunity to calculate the concentration of a cation ($[\text{M}^{n+}]$) without necessity to know exactly the concentration of a sensor according to Eq. (9),⁵

$$[\text{M}^{n+}] = K_D \frac{R - R_{\min}}{R_{\max} - R}, \quad (9)$$

where R is the ratio I_{340}/I_{440} for the studied sample with an unknown M^{n+} content, R_{\max} and R_{\min} correspond to the ratios I_{340}/I_{440} measured for the analyte bound and analyte free probe respectively, and K_D is the complex dissociation constant. For instance, the ratio of emission intensities R for the $6.5 \mu\text{M}$ solution of **BNI3** containing 2 equivalents of Ca^{2+} is 0.54. Assuming that R_{\min} and R_{\max} values are as high as 0.15 and 0.92 (found from the titration curve (Fig. 6b)) and $K_D = 1 / K = 1 / 10^{5.04} \text{ M}$ ($\lg K = 5.04$ for **(BNI3)·Ca²⁺**, Table 1), the equilibrium concentration of calcium cations in the solution is $[\text{Ca}^{2+}] = 9.4 \cdot 10^{-6} \text{ M}$. This value is very close to the one ($9.7 \cdot 10^{-6} \text{ M}$) obtained from the calculations of the solution composition using SPECFIT/32 program.

4. Conclusion

Novel crown-containing naphthalimide dyads **BNI2** and **BNI3** were synthesized based on convergent approach. The compounds were designed as ratiometric cation FRET chemosensors comprising PET switching amido-naphthalimide fluorophore linked with the amino-naphthalimide fragment. Steady-state and time-resolved optical studies revealed that the resonance energy transfer operating between the photoactive units competes fairly well with the photoinduced electron transfer from the crown ether receptor and, thus can be switched on by the presence of metal ions. As a result, a fluorescence enhancement of the acceptor amino-naphthalimide chromophore occurs upon the complex formation with Ca^{2+} and Mg^{2+} , the more pronounced effect being observed in the case of aza-15-crown-5-containing derivative **BNI3** where PET interaction was supposed to be stronger compared to **BNI2**.

In contrast to conventional “off–on” or “on–off” PET sensors with one fluorophore, our dyads open a way for ratiometric fluorescent detection of ions, because the FRET mediated “off–on” signal output obtained at $\lambda_{\text{ex}} = 340 \text{ nm}$ can be self-calibrated with respect to emission channel at $\lambda_{\text{ex}} = 440 \text{ nm}$ entirely unresponsive to the presence of analyte. Thus, the presented results have shown that compounds **BNI2** and **BNI3** can be of interest for the development of fluorescent ratiometric chemosensors for various kinds of cationic analysis. Due to versatile structural modification on the crown ether moiety, selective probes for various metal cations can be prepared. Related research is currently underway in our laboratory.

Acknowledgements

P.A.P. thanks RFBR project № 14-03-31935 (Design, synthesis, characterization of the compounds). O.A.F. thanks RFBR project № 15-03-04705 (Complex formation studies). G.J. thanks the Région Aquitaine for financial support.

Appendix. Supplementary Information

Supplementary data associated with this article can be found in the online version at doi

References

- 1 B. W. Van Der Meer, G. Coker and S. Y. S. Chen, *Resonance Energy Transfer: Theory and Data*, VCH, New York, 1994.
- 2 J. R. Lakowicz, *Principles of fluorescent spectroscopy*, Springer science + Business Media, LLC, Plenum Publishers, New York, 2006.
- 3 K. Kikuchi, H. Takakusa, T. Nagano, *Trends Anal. Chem.*, 2004, **23**, 407–415.
- 4 J. Fan, M. Hu, P. Zhan, X. Peng, *Chem. Soc. Rev.*, 2013, **42**, 29–43.
- 5 A. P. Demchenko, *Lab Chip*, 2005, **5**, 1210–1223.
- 6 L. Tolosa, K. Nowaczyk, J. Lakowicz, *An introduction to laser spectroscopy*, 2nd ed., Kluwer, New York, 2002.
- 7 L. G. F. Patrick, A. Whiting, *Dyes Pigm.*, 2002, **52**, 137–143.
- 8 I. Grabchev, R. Betsheva, *J. Photochem. Photobiol. A*, 2001, **142**, 73–78.
- 9 L. G. F. Patrick, A. Whiting, *Dyes Pigm.*, 2002, **55**, 123–132.
- 10 E. Martin, R. Weigand, A. Pardo, *J. Luminesc.*, 1996, **68**, 157–164.
- 11 W. W. Stewart, *J. Am. Chem. Soc.*, 1981, **103**, 7615–7620.
- 12 M. Sawa, T.-L. Hsu, T. Itoh, M. Sugiyama, S. R. Hanson, P. K. Vogt, C.-H. Wong, *PNAS*, 2006, **103**, 12371–12376.
- 13 H.-H. Lin, Y.-C. Chan, J.-W. Chen, C.-C. Chang, *J. Mater. Chem.*, 2011, **21**, 3170–3177.
- 14 S. Banerjee, E. B. Veale, C. M. Phelan, S. A. Murphy, G. M. Tocci, L. J. Gillespie, D. O. Frimannsson, J. M. Kelly, T. Gunnlaugsson, *Chem. Soc. Rev.*, 2013, **42**, 1601–1618.
- 15 W. Zhu, M. Hu, R. Yao, H. Tian, *J. Photochem. Photobiol. A*, 2003, **154**, 169–177.
- 16 G. Tu, Q. Zhou, Y. Cheng, Y. Geng, L. Wang, D. Ma, X. Jing, F. Wang, *Synth. Met.*, 2005, **152**, 233–236.
- 17 C. Coya, R. Blanco, R. Juárez, R. Gómez, R. Martínez, A. de Andrés, Á. L. Álvarez, C. Zaldo, M. M. Ramos, A. de la Peña, C. Seoane, J. L. Segura, *Eur. Polym. J.*, 2010, **46**, 1778–1789.

- 18 L. Song, E. A. Jares-Erijman, T. M. Jovin, *J. Photochem. Photobiol. A*, 2002, **150**, 177–185.
- 19 X. Meng, W. Zhu, Q. Zhang, Y. Feng, W. Tan, H. Tian, *J. Phys. Chem. B*, 2008, **112**, 15636–15645.
- 20 O. A. Fedorova, P. A. Panchenko, Y. V. Fedorov, F. G. Erko, J. Berthet, S. Delbaere, *J. Photochem. Photobiol. A*, 2015, **303–304**, 28–35.
- 21 I. Grabchev, I. Moneva, *J. Polym. Sci.*, 1999, **74**, 151–157.
- 22 Y. Zhang, W. Zhu, W. Wang, H. Tian, J. Su, W. Wang, *J. Mater. Chem.*, 2002, **12**, 1294–1300.
- 23 P. A. Panchenko, O. A. Fedorova, Y. V. Fedorov, *Russ. Chem. Rev.*, 2014, **83**, 155–182.
- 24 R. M. Duke, E. B. Veale, F. M. Pfeffer, P. E. Kruger, T. Gunnlaugsson, *Chem. Soc. Rev.*, 2010, **39**, 3936–3953.
- 25 N. I. Georgiev, V. B. Bojinov, P. S. Nikolov, *Dyes Pigm.*, 2009, **81**, 18–26.
- 26 N. I. Georgiev, V. B. Bojinov, N. Marinova, *Sens. Actuators B*, 2010, **150**, 655–666.
- 27 N. I. Georgiev, A. M. Asiri, A. H. Qusti, K. A. Alamry, V. B. Bojinov, *Sens. Actuators B*, 2014, **190**, 185–198.
- 28 X. Zhou, F. Su, H. Lu, P. Senechal-Willis, Y. Tian, R. H. Johnson, D. R. Meldrum, *Biomater.*, 2012, **33**, 171–180.
- 29 B. H. Shankar, D. Ramaiah, *J. Phys. Chem. B*, 2011, **115**, 13292–13299.
- 30 V. S. Jisha, A. J. Thomas, D. Ramaiah, *J. Org. Chem.*, 2009, **74**, 6667–6673.
- 31 Z. Zhou, M. Yu, H. Yang, K. Huang, F. Li, T. Yi, C. Huang, *Chem. Commun.*, 2008, 3387–3389.
- 32 V. B. Bojinov, A. I. Venkova, N. I. Georgiev, *Sens. Actuators B*, 2009, **143**, 42–49.
- 33 Q. Wang, C. Li, Y. Zou, H. Wang, T. Yi, C. Huang, *Org. Biomol. Chem.*, 2012, **10**, 6740–6746.
- 34 P. Mahato, S. Saha, E. Suresh, R. D. Liddo, P. P. Parnigotto, M. T. Conconi, M. K. Kesharwani, B. Ganguly, A. Das, *Inorg. Chem.*, 2012, **51**, 1769–1777.
- 35 Y. Liu, X. Lv, Y. Zhao, M. Chen, J. Liu, P. Wang, W. Guo, *Dyes Pigm.*, 2012, **92**, 909–915.
- 36 J. Fan, C. Lin, H. Li, P. Zhan, J. Wang, S. Cui, M. Hu, G. Cheng, X. Peng, *Dyes Pigm.*, 2013, **99**, 620–626.
- 37 J. Fan, P. Zhan, M. Hu, W. Sun, J. Tang, J. Wang, S. Sun, F. song, X. Peng, *Org. Lett.*, 2013, **15**, 492–495.
- 38 C.-Y. Li, Y. Zhou, Y.-F. Li, C.-X. Zou, X.-F. Kong, *Sens. Actuators B*, 2013, **186**, 360–366.

- 39 N. I. Georgiev, M. D. Dimitrova, A. M. Asiri, K. A. Alamry, V. B. Bojinov, *Dyes Pigm.*, 2015, **115**, 172–180.
- 40 K. A. Alamry, N. I. Georgiev, S. A. El-Daly, L. A. Taib, V. B. Bojinov, *J. Luminesc.*, 2015, **158**, 50–59.
- 41 P. A. Panchenko, Y. V. Fedorov, V. P. Perevalov, G. Jonusauskas, O. A. Fedorova, *J. Phys. Chem. A*, 2010, **114**, 4118–4122.
- 42 P. A. Panchenko, Y. V. Fedorov, O. A. Fedorova, B. A. Izmailov, V. A. Vasnev, V. V. Istratov, E. A. Makeeva, M. N. Romyantseva, A. M. Gaskov, *Mendeleev Commun.*, 2011, **21**, 12–14.
- 43 P. A. Panchenko, Y. V. Fedorov, O. A. Fedorova, G. Jonusauskas, *Dyes Pigm.*, 2013, **98**, 347–357.
- 44 P. A. Panchenko, Y. V. Fedorov, O. A. Fedorova, V. P. Perevalov, G. Jonusauskas, *Russ. Chem. Bull.*, 2009, **58**, 1233–1240.
- 45 S. Nad, M. Kumbhakar, H. Pal, *J. Phys. Chem. A*, 2003, **107**, 4808–4816.
- 46 C. L. Renschler, L. A. Harrah, *Anal. Chem.*, 1983, **55**, 798–800.
- 47 K. A. Connors, *Binding constants: the measurement of molecular complex stability*, John Wiley & Sons, New York, 1987.
- 48 M. T. Beck, I. Nagypál, *Chemistry of complex equilibria*, John Wiley & Sons, New York, 1990.
- 49 D. L. Perry, *Handbook of Inorganic Compounds*, CRC Press, Boca Raton, 2011.
- 50 P. O'Neill, S. Steenken, D. Schulte-Frohlinde, *J. Phys. Chem.*, 1975, **79**, 2773–2779.
- 51 T. Shida, Y. Nosaka, T. Kato, *J. Phys. Chem.*, 1978, **82**, 695–698.